Detecting precursory earthquake migration patterns using the pattern informatics method

Yi-Hsuan Wu,[1] Chien-chih Chen,[1] and John B. Rundle[2]

Received 8 July 2008; revised 25 August 2008; accepted 28 August 2008; published 8 October 2008.

[1] In this paper we analyze the evolution of seismic activity using a dynamic modification of the pattern informatics method. This method identifies locations that have systematic fluctuations in seismicity on PI maps. By investigating the evolution of hotspot configurations on the PI map and calculating the distance between hotspots and the epicenter of the impending large earthquake, a migrating pattern of (increasing or decreasing) precursory change in seismicity is revealed. We find that hotspots on the PI map appear increasingly closer to the epicenter as the time of the forthcoming earthquake is approached, implying the existence of an earthquake preparation process. The migration pattern and associated decreasing distance is confirmed by a stochastic test, and therefore we conclude that a preparation process prior to large earthquakes can be detected. **Citation:** Wu, Y.-H., C.-C. Chen, and J. B. Rundle (2008), Detecting precursory earthquake migration patterns using the pattern informatics method, *Geophys. Res. Lett.*, *35*, L19304, doi:10.1029/2008GL035215.

1. Introduction

[2] Earthquake migration remains one of the most intriguing seismicity patterns before large earthquakes, since the time it was proposed by *Mogi* [1968]. Most of the reported earthquake migration patterns are related to the fluid/magma movement in the volcanic areas [e.g., *Battaglia et al.*, 2005; *Kao et al.*, 2007]. Detecting such a small-scaled migration pattern requires a dense seismic network, together with precise information on earthquake locations. On the other hand, based on the critical point theory of earthquakes [e.g., *Rundle et al.*, 2000c; *Chen et al.*, 2006], it is believed that there is a large-scaled preparation process associated with stress accumulation and nucleation before a large earthquake, thus implying a migration pattern in seismicity around the source area of the large earthquake. However, there exists as yet no systematic methodology to investigate the temporal behavior of earthquake migration patterns before large earthquakes.

[3] Earthquake fault systems are characterized by complex dynamics, thus it is hard to understand the behavior of earthquakes without knowledge of the unobservable underlying dynamics [*Rundle et al.*, 2000a, 2000b; *Tiampo et al.*, 2002a]. An alternative approach is to develop methods based on analyzing the dynamics of space-time patterns of seismicity, together with the associated space-time correlations. These correlations are the observable manifestations of the time-dependent drift of a high-dimensional state vector in a phase dynamical system [*Fukunaga*, 1970; *Holmes et al.*, 1996; *Mori and Kuramoto*, 1997; *Rundle et al.*, 2000a; *Tiampo et al.*, 2002a] (see Figure 1). The pattern informatics method, which is an example of a phase dynamical measure, was originally proposed as a promising method to detect the characteristic precursory patterns before large threshold earthquakes. In this study, we modify the PI method to investigate the time- and space-varying patterns calculated from seismicity in a progressive series of change intervals. Using this modification, the earthquake migration patterns before large earthquakes can be clearly observed. This study therefore proposes a systematic approach to understanding the process of anomalous earthquake seismicity migration before large earthquakes.

2. PI Method and the Measure of Migration Pattern

[4] While there are a variety of ways in which the PI state vector can be defined, we use the following steps [*Rundle et al.*, 2000a; *Tiampo et al.*, 2002a, 2002b; *Chen et al.*, 2005; *Holliday et al.*, 2007]:

[5] The study region is first divided into boxes with size of $0.1^\circ \times 0.1^\circ$. The seismic intensity function $I(x_i, t_b, t)$ is defined as the average number of earthquakes with magnitude larger than the cutoff magnitude M_c that occur in a grid box x_i and its eight neighboring boxes (the Moore neighbors). For investigating the seismicity change of the system within an interval from t_1 through t_2, the seismic intensity change is then calculated as $\Delta I(x_i, t_b, t_1, t_2) = I(x_i, t_b, t_2) - I(x_i, t_b, t_1)$ and denoted by $\Delta I(x_i, t_b)$. The sampling reference time t_b is shifted from t_0, which usually means the beginning time of earthquake data, to t_1. Shifting t_b consequently produces a time series of $\Delta I_{x_i}(t_b)$ for each x_i. The temporal normalization, i.e., subtracting the temporal mean $\langle \Delta I_{x_i}(t_b) \rangle$ and dividing by the temporal standard deviation $\sigma(\Delta I_{x_i}(t_b))$, is then carried out, and we could get a temporally normalized intensity change $\Delta \tilde{I}(x_i, t_b)$. Similarly, for each t_b, the space series of $\Delta \tilde{I}(x_i, t_b)$ is spatially normalized furthermore. Consequently, we could get a spatiotemporally normalized intensity change $\Delta \hat{I}(x_i, t_b)$. For taking both seismic activation and quiescence into consideration, the absolute value of normalized intensity change $\Delta \hat{I}(x_i, t_b)$ is further taken. The temporal average of $|\Delta \hat{I}(x_i, t_b)|$, denoted by $\overline{|\Delta \hat{I}(x_i)|}$, is then computed at each location x_i. Finally, the mean squared change $P(x_i) \equiv \overline{|\Delta \hat{I}(x_i)|}^2$, indicating the occurrence probability of future threshold events, is computed. The color-coded "hotspots" with high $P(x_i)$ in a PI

[1]Department of Earth Sciences and Graduate Institute of Geophysics, National Central University, Jhongli, Taiwan.
[2]Center for Computational Science and Engineering, University of California, Davis, California, USA.

0094-8276/08/2008GL035215$05.00

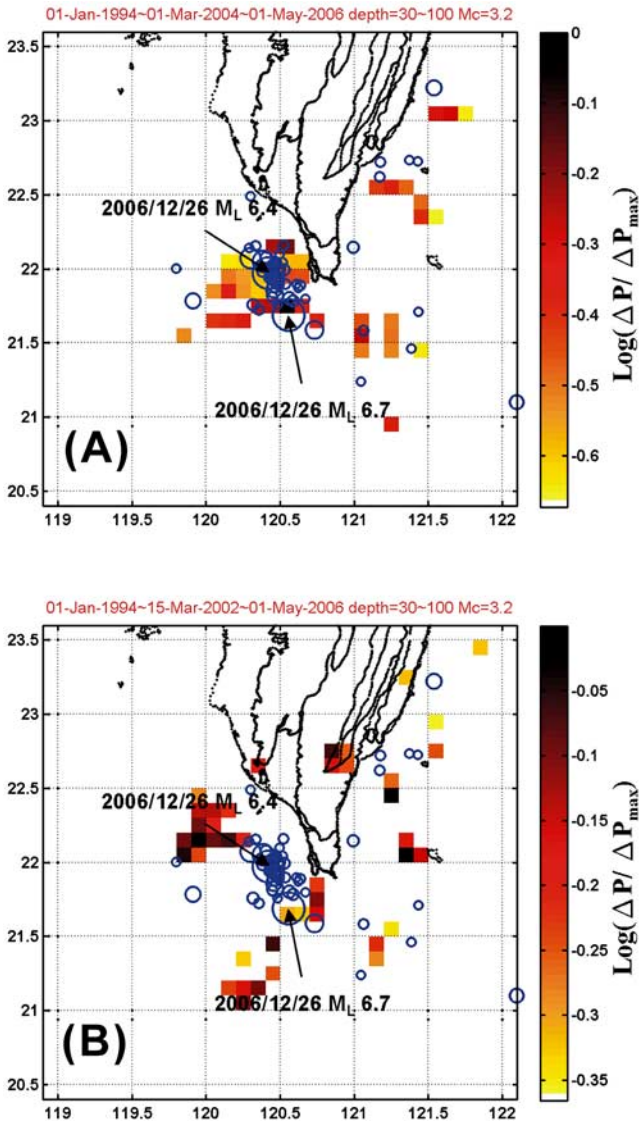

Figure 1. PI maps around the Pingtung doublet earthquakes calculated from the CWB catalogue with t_0 as 1994/01/01 and t_2 as 2006/05/01. Blue circles represent events larger than 4 that occurred after t_2. t_1 in the PI calculation are (a) 2004/03/01 and (b) 2002/03/15. Colored pixels (hotspots) represent areas with large seismicity changes caused by both the seismic activation and quiescence, indicating high probability for future large events.

map thus show the locations where the anomalous seismic activity occurred in the change interval of $\{t_1, t_2\}$. For example, as shown in Figure 1 is the retrospective PI analysis of the 2006 Pingtung (Taiwan) doublets with magnitudes of 6.7 and 6.4 by using t_1 as 2004/03/01 and 2002/03/15 in Figures 1a and 1b, respectively. The blue circles represent earthquakes occurred in a short span of six months after t_2 (= 2006/05/01). It is worth noticing that the colored pixels indicating high seismicity changes apparently migrate toward the source areas of the Pingtung doublets from 2002/03/15 (Figure 1b) through 2004/03/01 (Figure 1a). For the details of the retrospective PI analysis of the Pingtung doublets, we refer the readers to the paper by *Wu et al.* [2008].

[6] For demonstrating the earthquake migration pattern, now we propose a statistic to measure the *average* distance between the PI hotspots and target earthquakes, which is a measure of forecast error for a given configuration of PI hotspots. As shown in Figure 2a, the "error distance" ε_n is defined as the distance between the nth earthquake and the hotspot closest to it. The mean error distance $\langle\varepsilon\rangle$ is then defined by $\langle\varepsilon\rangle = \frac{1}{N}\sum_{n=1}^{N}\varepsilon_n$ for a set of target events. Since the number of hotspots is dependent on the decision threshold, the area A_H covered by hotspots would give a fraction $f = A_H/A$ of the map whereas the total area of the map is A. $\langle\varepsilon\rangle$ will decrease with increasing f which means lowering the threshold of hotspot plotting, as shown in Figure 2b, since more hotspot pixels appear in the PI map. For each t_1 in each specified change interval, a relation between $\langle\varepsilon\rangle$ and f (Figure 2b) thus gives the averaged distance ε_{area} (t_1) obtained by integrating the curve of $\langle\varepsilon\rangle$ versus f. Accordingly, the temporal evolution of anomalous seismic activity in space, i.e., the migration pattern, could be investigated by ε_{area} (t_1).

3. Results

[7] In this study, we used the earthquake catalogue maintained by the Taiwan Central Weather Bureau

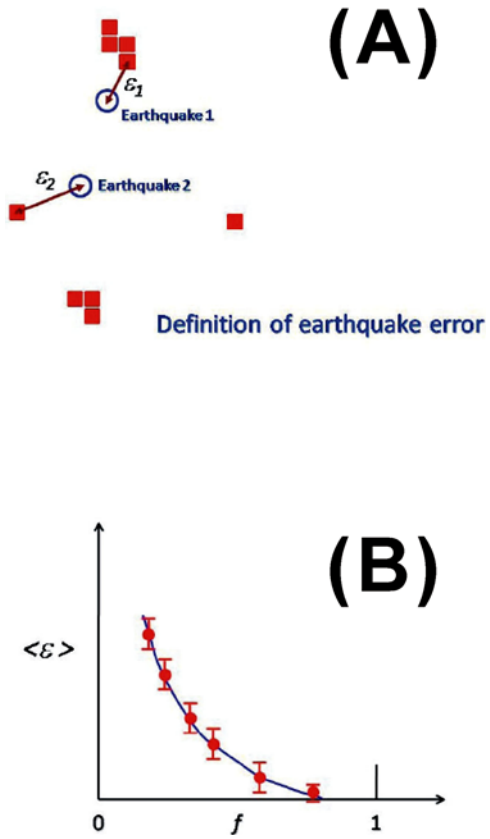

Figure 2. (a) Schematic diagram of the definition of error distance. The red blocks represent the hotspots in a PI map and the blue circles the locations of large earthquakes occurred after t_2. The error distance ε_n is the distance between the nth earthquake and the hotspot closest to it. (b) The relation between the mean error distance and the coverage fraction f of the PI hotspots.

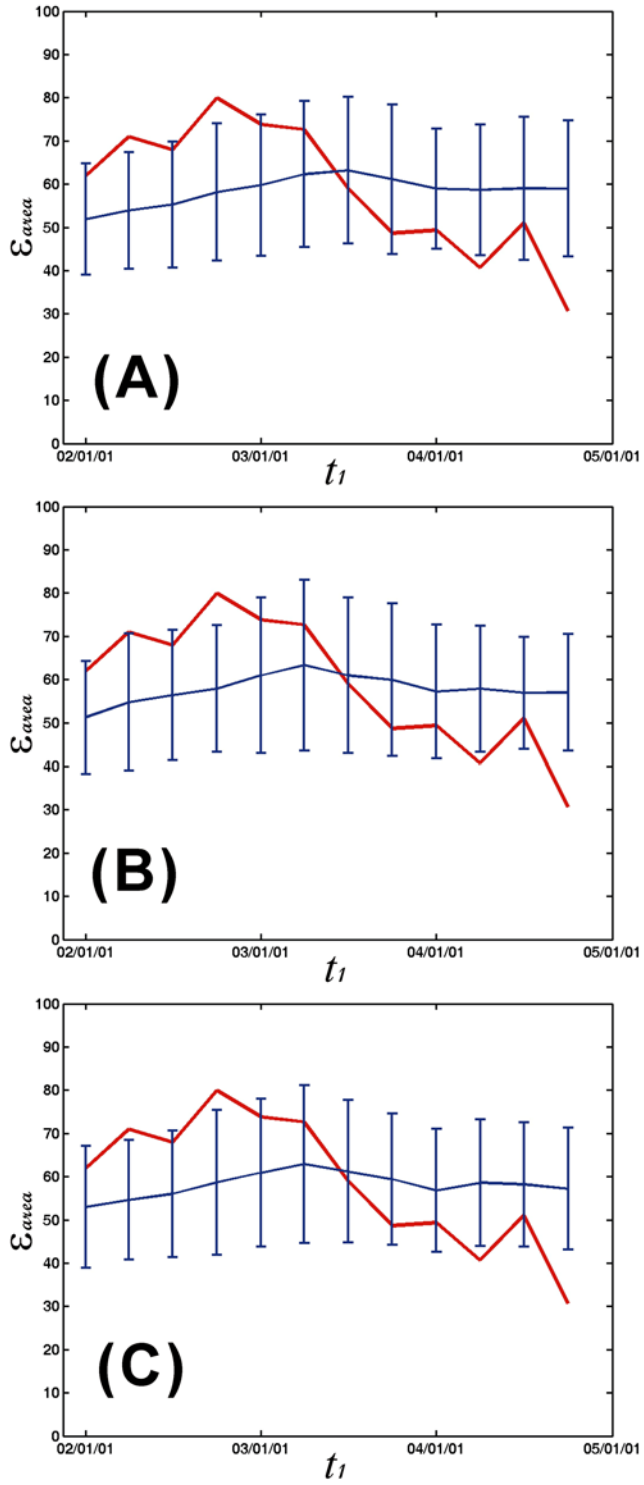

Figure 3. Curves of the integrated error distance ε_{area} (t_1) obtained by integrating the curve of $\langle\varepsilon\rangle$ versus f. The curves in red represent the results from the actual catalogue. The blue curves with error bars show the results after randomizing the catalogue in the (a) time-, (b) space-, and (c) both domains, respectively.

(CWB). We first consider the migration pattern for the 2006 Pingtung doublets. The Pingtung doublets struck a historically inactive region to the offshore southwestern Taiwan on 26 December 2006, where no earthquake with magnitude larger than five had occurred since 1973. The first event occurred at 8:26 p.m. (local time), then the second one occurred eight minutes later. Several undersea fiber-optic cables used to route internet traffic and telephone services between Taiwan and Asian area were seriously damaged.

[8] Events with magnitude larger than 3.2 and depth in the range 30 km to 100 km were used for this study. Again, for the selection criteria of earthquakes in the PI analysis, we refer the readers to the paper by *Wu et al.* [2008]. The result of error distance is shown as the red curve in Figure 3 by setting t_0 as 1994/01/01, t_2 as 2006/12/25, and t_1 shifting from 2002/01/01 to 2005/01/01 tri-monthly. The decreasing trend presented by the red curve in Figure 3 illustrates that the PI hotspots were genuinely getting closer to the hypocenters of the Pingtung sequence. That means the anomalous seismic activity (either increasing or decreasing activity) was approaching the source areas, as the time of the main shock approached. The slope obtained by fitting the decreasing linear trend is -0.0366 (kms/days). To provide a null hypothesis test, the curves in blue with error bars obtained by randomly shuffling the occurrence time, location, and both for the selected events from the catalogue in Figures 3a, 3b, and 3c, respectively, all show flat trends. After 500 realizations of randomizing both the occurrence time and location (Figure 3c), the mean slope of fitted linear trend in ε_{area} (t_1) and its standard deviation are 0.0031 (kms/days) and 0.019 (kms/days), respectively. Therefore, we confirm observation of the seismicity migration pattern before the Pingtung doublets at the 95% confidence level.

[9] We are also interested in analyzing the migration pattern of the 1999 Mw 7.6 Chi-Chi earthquake, by using the same strategy. Figure 4 shows our results for the Chi-Chi case. The events with magnitude larger than 3.5 and within the depth of 20 km were selected from CWB catalogue, whereas t_0 and t_2 were fixed at 1980/01/01 and 1999/06/30, respectively. For the selection criteria of earthquakes in the PI analysis of the Chi-Chi case, we refer the readers to the paper by *Chen et al.* [2005]. Then, we could explore the evolution of PI patterns with time by considering different t_1 into calculation. Two examples of PI maps are shown in Figures 4a and 4b with t_1 as 1992/12/23 and t_1 as 1998/7/25, respectively. Similar to the Pingtung case, the PI hotspots far from the epicenter in Figure 4a become closer to the source areas of the Chi-Chi sequence in Figure 4b, indicating the migration process. Again, a decreasing trend of the migration pattern can be found in the error distance calculation for the case of Chi-Chi earthquake. As shown in Figure 4c, the slope of the red curve obtained from the actual earthquake catalogue is -0.0146 (pixels/days). We also did the null hypothesis test for the Chi-Chi case. The mean slope obtained from 500 realizations of spatiotemporally randomizing the selected events is 0.874×10^{-5} (pixels/days), together with a standard deviation of 0.0074 (pixels/days). Only 4 out of 500 have the slopes smaller than the actual one. Again we observe, the slope data indicate that at the 95% confidence level, the seismicity migration to the source area of the Chi-

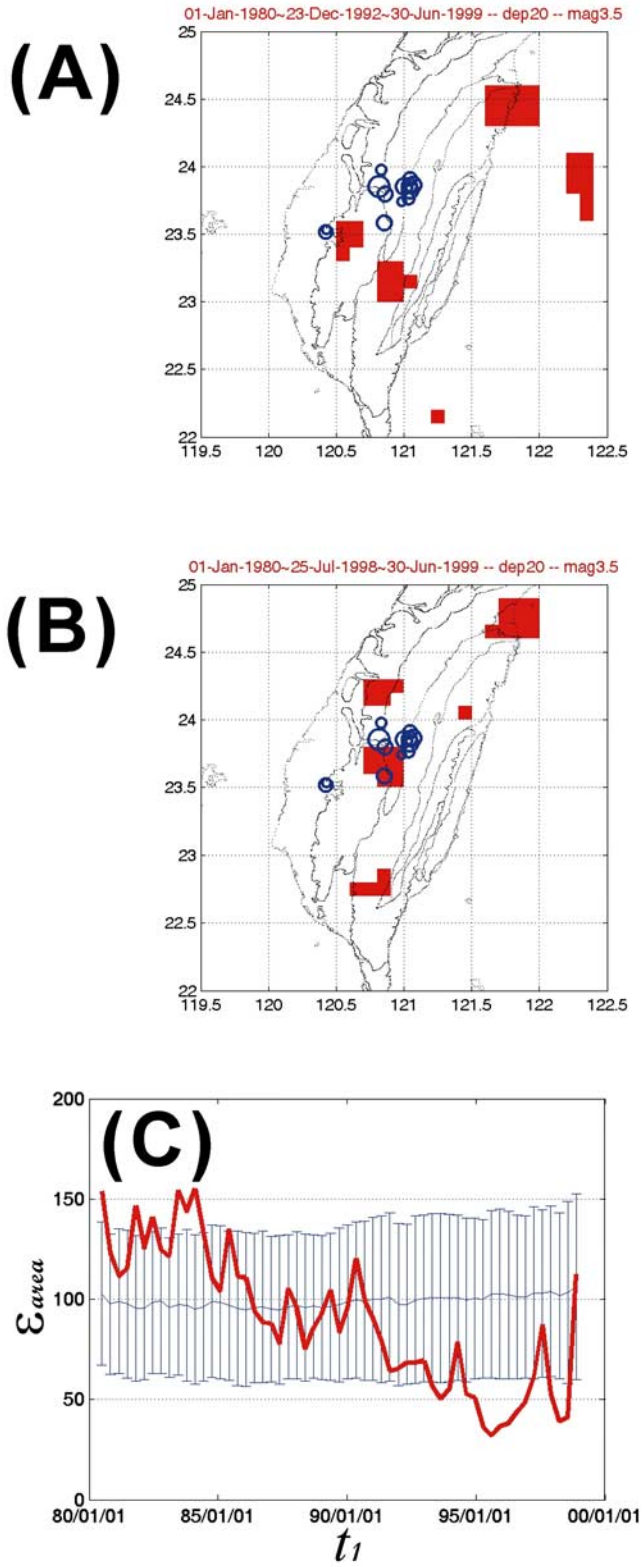

Figure 4. (a and b) are PI maps around the Chi-Chi earthquake. Blue circles represent earthquakes larger than 6 that occurred after t_2, which is 1999/06/30. PI hotspots represent areas with large seismicity changes. (c) Red curve of integrated error distance ε_{area} (t_1) represents the result obtained from real catalogue. Blue curve with error bars shows the results of spatiotemporally randomizing the catalogue.

Chi sequences cannot be obtained by chance from randomizing the catalogue.

4. Discussion and Conclusions

[10] Since the PI map is derived by computing the seismicity rate changes in the change interval relative to the background seismicity, the change interval plays an important role in the PI calculation. As shown in Figures 1 and 4, the PI pattern evolved in space over the different change intervals, leading us to examine the associated seismicity changes over time. We found the PI hotspots associated with intense seismicity changes were approaching closer to the source areas of the forthcoming large earthquakes, for instance, from Figure 1b through Figure 1a for the Pingtung sequence and from Figure 4a through Figure 4b for the Chi-Chi event. Observations such as these are reminiscent of the so-called earthquake migration process [*Mogi*, 1968, 1969, 1981, 1985; *Rydelek and Sacks*, 2001; *Battaglia et al.*, 2005; *Kao et al.*, 2007].

[11] Migration of seismic activity can be produced by different physical processes, requiring considerations from both seismological and tectonic viewpoints. For example, a prominent migration pattern was observed in a series of large earthquakes ($M \geq 7.5$) moving down the Japan Trench from north to south at intervals of 2 or 3 years in the 1930's and was understood as the development of large-scale fracturing along the trench [*Mogi*, 1969, 1985]. The appearance of the doughnut pattern exhibited by earthquakes with magnitude larger than 3.0 around the area of the Izu Peninsula was hypothesized to be a preparation process prior to the forthcoming large earthquake [*Mogi*, 1981, 1985]. During the preparation process of crack nucleation, these ideas imply that seismicity will tend to migrate towards the direction in which the fault grows [*Scholz*, 2002].

[12] In this study we demonstrated that the migration trend of seismicity can be observed by calculating the average error distance between hotspots and target epicenters. The ε_{area} (t_1) curves in Figures 3 and 4c show that the distances between target epicenters and PI hotspots became smaller and smaller as the times of the major Pingtung and Chi-Chi earthquakes approached. Our findings thus suggest that migration of seismic activity may exist before large earthquakes and migration toward the source area of the events might be caused by a nucleation process. In many previous works on earthquake migration, researchers have provided different algorithms to detect the migration process, usually by sophisticated calculations of stress and strain [e.g., *Stein*, 1999; *Niu et al.*, 2003; *Rydelek and Sacks*, 2001] that are difficult to observe in nature. By contrast, the results of the migration pattern in this study were obtained by an easy and direct calculation of seismicity rate changes. We propose that earthquake rate changes revealed by the PI method might find considerable use as a type of earthquake "stress meter" [e.g., *Dieterich et al.*, 2000; *Chen et al.*, 2006], allowing the detection of space-time migration patterns before large earthquakes and consequently, leading to new advances in our understanding of earthquake physics.

[13] **Acknowledgments.** The effort of the Central Weather Bureau (CWB) of Taiwan to maintain the CWB Seismic Network is highly appreciated. We are also grateful for research supports from the National Science Council (ROC) and the Department of Earth Sciences at National Central University (ROC). JBR would also like to acknowledge generous support from NASA, in particular from grant NNX08AF69G to the University of California, Davis.

References

Battaglia, J., V. Ferrazzini, T. Staudacher, K. Aki, and J.-L. Cheminee (2005), Pre-eruptive migration of earthquakes at the Piton de la Fournaise volcano (Reunion Island), *Geophys. J. Int.*, *161*, 549–558.

Chen, C.-C., J. B. Rundle, J. R. Holliday, K. Z. Nanjo, D. L. Turcotte, S.-C. Li, and K. F. Tiampo (2005), The 1999 Chi-Chi, Taiwan, earthquake as a typical example of seismic activation and quiescence, *Geophys. Res. Lett.*, *32*, L22315, doi:10.1029/2005GL023991.

Chen, C.-C., J. B. Rundle, H.-C. Li, J. R. Holliday, D. L. Turcotte, and K. F. Tiampo (2006), Critical point theory of earthquakes: Observation of correlated and cooperative behavior on earthquake fault systems, *Geophys. Res. Lett.*, *33*, L18302, doi:10.1029/2006GL027323.

Dieterich, J., V. Cayol, and P. Okubo (2000), The use of earthquake rate changes as a stress meter at Kilauea volcano, *Nature*, *408*, 457–460.

Fukunaga, K. (1970), *Introduction to Statistical Pattern Recognition*, Academic, New York.

Holliday, J. R., C.-C. Chen, K. F. Tiampo, J. B. Rundle, D. L. Turcotte, and A. Donnelan (2007), A RELM earthquake forecast based on pattern informatics, *Seismol. Res. Lett.*, *78*, 87–93.

Holmes, P., J. L. Lumley, and G. Berkooz (1996), *Turbulence, Coherent Structures, Dynamical Systems and Symmetry*, Cambridge Univ. Press, Cambridge, U. K.

Kao, H., S.-J. Shan, G. Rogers, and H. Dragert (2007), Migration characteristics of seismic tremors in the northern Cascadia margin, *Geophys. Res. Lett.*, *34*, L03304, doi:10.1029/2006GL028430.

Mogi, K. (1968), Source locations of elastic shocks in the fracturing process in rocks, *Bull. Earthquake Res. Inst. Univ. Tokyo*, *46*, 1103–1125.

Mogi, K. (1969), Some features of recent seismic activity in and near Japan (2): Activity before and after great earthquakes, *Bull. Earthquake Res. Inst. Univ. Tokyo*, *47*, 395–417.

Mogi, K. (1981), Seismicity in western Japan and long-term earthquake forecasting, in *Earthquake Prediction*, *Maurice Ewing Ser.*, vol. 4, edited by D. W. Simpson and P. G. Richards, pp. 43–51, AGU, Washington, D. C.

Mogi, K. (1985), *Earthquake Prediction*, Academic, Tokyo.

Mori, H., and Y. Kuramoto (1997), *Dissipative Structures and Chaos*, Springer, New York.

Niu, F., P. G. Silver, R. M. Nadeau, and T. V. McEvilly (2003), Migration of seismic scatterers associated with the 1993 Parkfield aseismic transient event, *Nature*, *426*, 544–548.

Rundle, J. B., W. Klein, K. Tiampo, and S. Gross (2000a), Linear pattern dynamics in nonlinear threshold systems, *Phys. Rev. E*, *61*, 2418–2432.

Rundle, J. B., W. Klein, S. Gross, and K. F. Tiampo (2000b), Dynamics of seismicity patterns in systems of earthquake faults, in *Geocomplexity and the Physics of Earthquakes*, *Geophys. Monogr. Ser.*, vol. 120, edited by J. B. Rundle, D. L. Turcotte, and W. Klein, pp. 127–146, AGU, Washington, D. C.

Rundle, J. B., W. Klein, D. L. Turcotte, and B. D. Malamud (2000c), Precursory seismic activation and critical-point phenomena, *Pure Appl. Geophys.*, *157*, 2165–2182.

Rydelek, P. A., and I. S. Sacks (2001), Migration of large earthquakes along the San Jacinto fault; stress diffusion from the 1857 Fort Tejon earthquake, *Geophys. Res. Lett.*, *28*, 3079–3082.

Scholz, C. H. (2002), *The Mechanics of Earthquakes and Faulting*, 2nd ed., Cambridge Univ. Press, Cambridge, U. K.

Stein, R. S. (1999), The role of stress transfer in earthquake occurrence, *Nature*, *402*, 605–609.

Tiampo, K. F., J. B. Rundle, S. McGinnis, S. J. Gross, and W. Klein (2002a), Mean-field threshold systems and phase dynamics: An application to earthquake fault systems, *Europhys. Lett.*, *60*, 481–487.

Tiampo, K. F., J. B. Rundle, S. McGinnis, and W. Klein (2002b), Pattern dynamics and forecast methods in seismically active regions, *Pure Appl. Geophys.*, *159*, 2429–2467.

Wu, Y.-H., C.-C. Chen, and J. B. Rundle (2008), Precursory seismic activation of the Pingtung (Taiwan) offshore doublet earthquakes on December 26, 2006: A pattern informatics analysis, *Terr. Atmos. Ocean. Sci.*, in press.

C.-C. Chen and Y.-H. Wu, Graduate Institute of Geophysics, National Central University, Jhongli, Taoyuan 320, Taiwan. (chencc@ncu.edu.tw)

J. B. Rundle, Center for Computational Science and Engineering, University of California, One Shields Avenue, Davis, CA 95616, USA.